JPP Journal of Pharmacy and Pharmacology

JPP 2004, 56: 1379–1387

Received June 2, 2004
Accepted August 5, 2004
DOI 10.1211/0022357044751
ISSN 0022-3573

Griseofulvin micronization and dissolution rate improvement by supercritical assisted atomization

E. Reverchon, G. Della Porta, A. Spada and A. Antonacci

Abstract

Supercritical assisted atomization (SAA) was used to micronize griseofulvin (GF), selected as a model compound, to verify the performance of this innovative process. SAA is based on the solubilization of supercritical carbon dioxide in a liquid solution containing the drug. The ternary mixture is then sprayed through a nozzle and microparticles are formed as a consequence of the enhanced atomization. Precipitation temperature and drug concentration in the liquid solution were studied to evaluate their influence on morphology and size of precipitated particles. A good particle size control was obtained and GF spherical particles with mean diameters ranging from 0.5 to 2.5 μm were produced with a narrow particle size distribution. Processed GF was characterized by high-performance liquid chromatography-UV/vis, headspace-gas chromatography-flame ionization detection, differential scanning calorimetry, BET and X-ray analyses. No drug degradation was observed and a solvent residue (acetone) less than 800 ppm was measured. GF microparticles showed good stability and surface areas ranging from about 4 to 6 $m^2 g^{-1}$; moreover, the micronized drug retained the crystalline habit. GF capsules were formulated with starch and used to compare the dissolution rate of SAA-processed and conventional jet-milled drug. A faster dissolution and a better reproducibility of the dissolution profile were observed for SAA-processed GF.

Introduction

Griseofulvin (GF) is a well known antibiotic and antifungal agent. It is widely used but because its therapeutic dose is close to the toxicity limit, GF preparations have to be carefully designed for maximum absorption. The main problem is the low GF solubility in water (approx. 15 $\mu g\,mL^{-1}$ at 37°C) and, therefore, poor bioavailability and incomplete absorption through the gastrointestinal tract are obtained (Gull & Trinci 1973; Lin et al 1973). This is a problem for all hydrophobic drugs: the dissolution rate is the limiting step for the uptake of the drug after oral administration. It is also well known that a decrease in particle size results in a greater dissolution rate (Mosharraf & Nystrom 1995).

Conventional methods for micrometric particle generation usually do not assure an efficient control of the particle size: they sometimes produce thermal degradation or drug contamination, and reproducibility problems among different batches have been observed. Several micronization processes based on supercritical fluids (SCF) have been proposed to overcome these limitations. SCF can take advantage of some specific properties of gases at supercritical conditions. They are characterized by a continuous adjustable solvent power/selectivity obtained by varying pressure and temperature. Moreover, their diffusivities can be about two orders of magnitude greater than those of liquids. As a result, SCF-based processes can show very fast mass transfer and performances that cannot be obtained by conventional solvents.

The most studied SCF-based micronization techniques are: rapid expansion of supercritical solutions (RESS) (Matson et al 1987; Reverchon et al 1995), particles generation from gas saturated solutions (Sencar-Bozic et al 1997; Kerc et al 1999), and supercritical antisolvent precipitation (SAS) (Bleich et al 1994; Subramaniam et al 1997; Reverchon & Della Porta 1999; Rehman et al 2000).

GF micronization by RESS using supercritical trifluoromethane has been attempted (Reverchon et al 1995; Turk et al 2002). The drug was dissolved in the

Dipartimento di Ingegneria Chimica e Alimentare, Università di Salerno, Via Ponte Don Melillo, 84084 Fisciano (SA), Italy

E. Reverchon, G. Della Porta, A. Spada, A. Antonacci

Correspondence: E. Reverchon, Dipartimento di Ingegneria Chimica e Alimentare, Università di Salerno, Via Ponte Don Melillo, 84084 Fisciano (SA), Italy. E-mail: ereverchon@unisa.it

Acknowledgements and funding: The authors would like to thank Dr Raffaele Annaloro and Dr Stefano Conti from Italchimici SPA (Pomezia, Rome, Italy) for capsule formulation and for help in optimizing the dissolution test. The authors acknowledge MiUR (Italian Ministry for University and Research) for partial financial support of this research (2003).

SCF, then a fast depressurization produced GF precipitation and solid particles were obtained. RESS experiments were performed at different operating conditions and needle-like crystals ranging from 1 to 10 μm were produced (Reverchon et al 1995). Particles ranging from 200 to 300 nm were also produced by Turk et al (2002), which showed an improvement in the dissolution rate but a very low process yield.

GF micronization was also attempted by SAS using supercritical carbon dioxide (SC-CO_2). This process is based on drug solubilization in a liquid solvent: the solution is then sprayed in a high-pressure vessel containing the SCF. The liquid solvent and the SCF form a solution and the drug precipitates. Reverchon & Della Porta (1999) attempted GF precipitation from *N*-methyl pyrrolidone. The process was not successful because of the almost complete extraction of the drug. GF extraction was attributed to the formation of a solvato complex that increases the drug solubility in the supercritical antisolvent producing a co-solvent effect. Some millimetre-long needle-like crystals were produced when dichloromethane and dimethylsulfoxide were used as liquid solvents owing to the formation of a liquid phase at the bottom of the precipitation vessel. Using SAS, Foster et al (2003) produced GF needle-like particles ranging from 1 μm to some millimetres using organic solvents such as acetone, ethanol and dimethylformamide. These authors also indicated that the re-processing of GF by SAS improved the dissolution rate in comparison with unprocessed GF.

Chattopadhyay & Gupta (2001) used a modified SAS process called supercritical antisolvent precipitation with an enhanced mass transfer (SAS-EM). They introduced a vibrating ultrasonic device in the precipitator to improve mass transfer during the micronization process, increasing the mixing and decreasing the agglomeration of particles. They reported the formation of GF microparticles with different size and morphologies when the vibration intensity was varied.

Various SC-CO_2 assisted atomization processes have also been proposed. Particularly, Sievers and co-workers proposed the SC-CO_2 assisted nebulization (CAN-BD): they produced an aerosol from the mixing (not solubilization) of SC-CO_2 and the liquid solvent using a near-zero volume tee and various capillary injectors (Sievers et al 1998; Sellers et al 2001). Ventosa et al (2001) proposed the depressurization of an expanded liquid organic solution crystallization (DELOS) technique, which uses the simple batch depressurization of a solution contacted by SC-CO_2.

We recently proposed supercritical assisted atomization (SAA) (Reverchon 2002, 2003; Reverchon & Della Porta 2003a, b, c; Reverchon et al 2003). In this process, a thermostated packed contactor is used to obtain a continuous near-equilibrium solubilization of SC-CO_2 in the liquid solution. The solution, rapidly formed in the contacting device, is then sprayed into the precipitator at atmospheric pressure. A two-step atomization is obtained: the primary droplets at the outlet of the injector are further divided in secondary droplets owing to SC-CO_2 expansion from the inside of the primary ones. One of the specific expectations of using SCF instead of gas is its enhanced mass transfer properties. Indeed, as a rule, gases that are not at supercritical conditions are released slowly from the liquid phase and their contribution to a two-step atomization is not relevant (Liu 1999). We discovered that gases at supercritical conditions are released from the liquid phase in a faster process: therefore, SC-CO_2 can effectively contribute to the second atomization step (Reverchon 2003).

To date, the GF micronization by SCF has been only partly successful. The aim of the present study was to micronize GF by SAA, considering this drug as a model of poorly water-soluble pharmaceutical compounds and to verify the performance of SAA. Different SAA process parameters can be studied to obtain good size control: SCF/liquid mass flow ratio, precipitation temperature and drug concentration in the liquid solution. The effects of these process parameters on particle morphology, size and size distribution can be monitored. Indeed, several aspects related to an overall interpretation of the SAA process are still missing and information is only available on a limited number of compounds. Phase equilibria involved in the process can also play a relevant role. Moreover, apart from the solute and liquid solvent used, no general rules have been given until now about the SCF processability of drugs.

SAA-processed GF was analysed to evaluate its degradation, solvent residue, crystalline habit, stability and surface area. GF capsules formulated using the SAA-treated and the conventional jet-milled drug were used to study the dissolution rates and the resultant improvement of the drug bioavailability after SAA processing.

Materials and Methods

SAA apparatus

The SAA apparatus consists of two high-pressure pumps (model 305; Gilson) that deliver the liquid solution and CO_2 to a heated bath (Forlab model TR12; Carlo Erba) and then to the saturator. The saturator is a high-pressure vessel (50 cm^3) loaded with stainless steel perforated saddles that ensures a large contact surface between liquid solution and CO_2, thus enhancing the dissolution of the gaseous stream in the liquid solution. Residence times in the saturator can vary from several seconds to minutes at the commonly adopted process conditions. The solution obtained in the saturator is sprayed through a thin-wall 80-μm diameter injection nozzle into the precipitator.

N_2 is taken from a cylinder, heated in an electric heat exchanger (model CBEN 24G6; Watlow) and sent to the precipitator to assist evaporation of the liquid droplets. The precipitator is a stainless steel vessel (3 dm^3) operating at atmospheric pressure. The saturator and the precipitator are electrically heated using thin band heaters. A stainless steel frit at the bottom of the precipitator allows the powder collection and the gaseous stream flow out. A condenser located after the precipitator is used to recover the liquid solvent. Manometers, temperature controllers

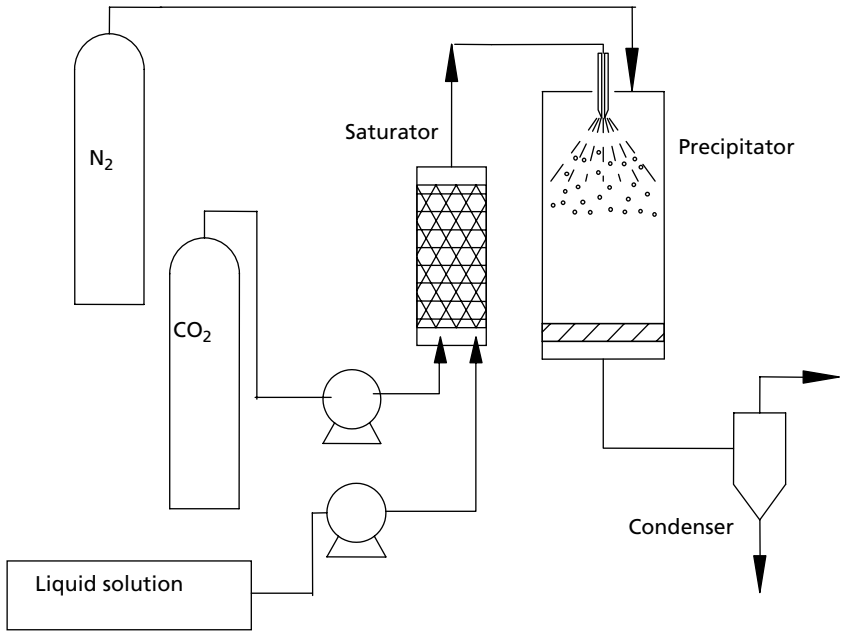

Figure 1 Schematic representation of the supercritical assisted atomization apparatus.

and thermocouples complete the apparatus. The SAA layout is shown in Figure 1. Further details have been published elsewhere (Reverchon 2002). Forty SAA experiments were performed, varying the different process parameters, and each successful run was replicated. The typical SAA yield is 95%; the material lost is related to the difficulty in recovering the powder on the walls of the precipitation vessel.

Materials

GF (purity 98%) was supplied by Sigma-Aldrich (Milano, Italy). Water, methanol and acetone (high-performance liquid chromatography (HPLC) grade) were supplied by Carlo Erba Reagenti (Milan, Italy). Carbon dioxide and nitrogen (CO_2, N_2) were purchased from SON (Naples, Italy). Untreated GF consisted of irregular crystals with particle sizes ranging from 10 to 100 μm. Jet-milled GF was supplied by Microgrinding S.A. (Lugano, Switzerland) and consisted of micronic crystals with particle sizes ranging from 0.5 to 10 μm.

Powder morphology by scanning electron microscopy (SEM)

GF powders, sampled at different heights in the precipitation chamber, were observed by SEM (model 420; LEO). Powders were dispersed on a carbon tab previously stuck to an aluminium stub (Agar Scientific, UK). Samples were coated with gold-palladium (layer thickness 250Å) using a sputter coater (model 108A; Agar Scientific). At least 30 SEM images were taken for each run to verify the powder uniformity.

Particle size distribution

Particle size and particle size distribution were evaluated from SEM images using the Sigma Scan Pro Software (release 5.0; Jandel Scientific); approximately 1000 particle diameters were considered in each particle size distribution calculation. Histograms representing the particle size distribution were best fitted using Microcal Origin Software (release 5.0; Microcal Software Inc.). Log–normal curves giving a reasonably good representation of the non-symmetric distributions were obtained.

Statistical analysis

Statistical analysis was performed using CoStat version 6.2 software (CoHort Software, USA). The differences in the thermodynamic properties of the various samples analysed by differential scanning calorimetry (DSC) were statistically evaluated using one-way analysis of variance. The individual differences between the samples were examined using the Newman–Keuls test. The percentages of dissolved drug at different time points for SAA and jet-milled GF were examined using the Mann–Whitney *U*-test. All tests were performed using a significance level of 0.05.

Drug degradation

Drug degradation was evaluated by performing HPLC-UV/vis (model G131-132; Hewlett Packard) analysis on untreated and SAA-processed GF according to the procedure suggested by Quanyun & Lawrence (1999). The elution was obtained using a reverse phase C18 column (4.6 × 250 mm; 5 μm particle size; 80 Å pore size; Hypersyl ODS). The column was equilibrated at a flow

rate of 1 mL min^{-1} with a mobile phase consisting of methanol and water (70:30). The drug was monitored at 291 nm with a retention time of 26.4 min. All chromatographic analyses were carried out at room temperature. The average column back pressure was approximately 15 MPa. Analyses were performed on each batch of processed GF in replicate.

Solvent residue

Acetone residue was measured by a headspace sampler (model 50 SCAN; Hewlett Packard, USA) coupled to a gas chromatograph interfaced with a flame ionization detector (GC-FID). Acetone was separated using a fused-silica capillary column (model DB-1; J&W, Folsom, USA): 30 m length, 0.25 mm internal diameter, 0.25 μm film thickness. GC conditions were: oven temperature at 40°C for 8 min. The injector was maintained at 180°C (split mode, ratio 1:1) and helium was used as the carrier gas (7 mL min^{-1}). Headspace conditions were: equilibration time 60 min at 100°C, pressurization time 2 min, loop fill time 1 min. Headspace samples were prepared in 10-mL vials filled with 50 mg of drug. Analyses were performed on each batch of processed GF in replicate.

Solid state

Solid state analysis of the samples was performed using an X-ray powder diffractometer (model D8 Discover; Bruker, USA) with a Cu sealed tube source. Samples were placed in the holder and flattened with a glass slide to ensure a good surface texture. The measuring conditions were: Ni-filtered CuKα radiation, $\lambda = 1.54$ Å, 2θ angle ranging from 20° to 70° with a scan rate of 3 s/step and a step size of 0.2°. Analyses were performed on several GF batches produced at different SAA process conditions.

Degree of crystallinity and drug stability

The degree of crystallinity of GF was measured using DSC (model TC11; Mettler, USA), according to the method proposed by Ahmed et al (1998). Temperature and enthalpy of fusion were calibrated with indium standard materials (melting point 156.6°C). The GF sample (5 ± 0.5 mg) was accurately weighed, crimped in an aluminium pan and heated from to 25°C to 300°C under a nitrogen purge at 10°C min^{-1}. Drug stability was evaluated by DSC analyses performed on different GF batches produced by SAA. Each batch was analysed again after 6 days of storage in air with a relative humidity of 60% to evaluate any re-crystallization events.

Surface area

Specific surface area measurements were performed using a sorptometer (model COSTECH 1040; Fisons Instruments, USA). Measurements were carried out on the untreated GF and on different GF micronized batches by nitrogen adsorption at −196°C, after sample pre-treatment in helium flow for 1 h at 100°C.

Capsule preparation and dissolution rate

GF capsules were prepared according to the US Pharmacopeia (2003). Gelatine capsules (Qualicaps 0.45 mL) were manually prepared mixing 50 mg of GF (jet-milled or SAA micronized) and 50 mg of maize starch. Tests were performed with an automatic dissolution test apparatus (Sotax AT 7 Off-line) using 1000 mL of distilled water mixed with 5.4 mg of sodium lauryl sulfate stirred at 50 rev min^{-1} at 37°C (±0.5°C). A 10-mL volume of solution was sampled every 5 min and replaced with an equal amount of dissolution fluid. The samples were filtered through a 0.2-μm membrane filter (Millex-GV PVDF Durapore) and photometrically assayed at 291 nm with a UV/vis spectrophotometer (PerkinElmer Lambda 35). The calibration curve was produced using six different solutions. The dissolution test was performed in six replicates for each batch of capsules.

Results and Discussion

Selection of the saturator operating parameters

The solubilization of SC-CO_2 in the liquid solution inside the saturator is one of the key parameters controlling the efficiency of the SAA process. CO_2 solubility in the liquid depends on the liquid solvent chosen, temperature, pressure and residence time in the saturator, since it is related to high pressure vapour–liquid equilibria (Reverchon 2002).

In the present work, acetone was selected as the liquid solvent because it has a low toxic potential (Federal Register 1997) and GF has good solubility in this solvent (30 mg mL^{-1} at room temperature). Data on high pressure vapour–liquid equilibria for the binary system acetone/CO_2 were found in the literature (Ohe 1990; Chang et al 1997). Operating pressure and temperature were explored over the pressure range 7–9 MPa and over the temperature range 70–90°C. To obtain in the saturator a single liquid phase located to the left of the mixture critical point, we assumed that the presence of the GF does not modify the miscibility behaviour of the acetone/CO_2 system. In preliminary experiments, the best results in terms of stability of the process and GF precipitated particles were observed at 8 MPa and 80°C. These pressure and temperature conditions were therefore used in all the experiments proposed in this work.

Selection of the mass flow ratios for CO_2/liquid solution

When pressure and temperature are fixed, the mass flow ratio corresponds to a given operating point in the ternary vapour–liquid equilibrium diagram of the system drug/CO_2/liquid solvent. However, quantitative vapour–liquid equilibrium data at high pressure on ternary systems is still missing and this thermodynamic data is difficult to determine. We tried to operate at pressure and temperature conditions that ensure the complete miscibility for the

binary system solvent/CO_2. However, in the case of the ternary system (drug/solvent/CO_2) the vapour–liquid equilibrium could be significantly modified by the presence of the third component (we frequently observed the formation of two phases). Making a rough approximation, we can assume that the modification of the binary system vapour–liquid equilibrium owing to the presence of solute can consist of the shift of the critical point of the mixture to higher pressures. Therefore, at least an empirical study of the effect of the mass flow ratio for the given ternary system is always necessary.

The mass flow ratios between CO_2 and liquid solution explored in this work were: 1.2, 1.5 and 1.9. These mass flow ratio values correspond to molar fractions of CO_2 in the liquid solution of 0.61, 0.66 and 0.71, respectively, calculated in the hypothesis that all CO_2 sent to the saturator dissolves in the liquid. The CO_2 flow rate commonly used was 9.9 mL min^{-1} and the liquid flow rate was set as a result. Usually, 100 mL of liquid solution was injected in each run.

When mass flow ratio values of 1.5 and 1.9 were used, the injector was always blocked and the SAA process failed. This problem occurs when GF precipitates inside the saturator and it can be explained with the shift of the acetone/CO_2 system into a vapour–liquid equilibrium region where two phases in equilibrium exist. In this case, a gas phase, containing part of the solvent and of the solute, is also formed and induces a partial solute precipitation in the saturator. Moreover, the precipitation of GF in the solvent-rich phase owing to the solubilization of CO_2 can also be responsible for the GF precipitation (De Gioannis et al 2004). This problem was not observed during the experiments performed at a mass flow ratio = 1.2. Therefore, this feed ratio was adopted in all the experiments performed in the following part of the work.

Effect of temperature in the precipitation chamber

Temperature optimization in the precipitation chamber is required to assist droplet evaporation and, at the same time, to minimize the stress on the treated drug. Preheated N_2 with a flow rate of 800 Ndm^3 h^{-1} is used to set the precipitation chamber at the desired temperature. The effect of temperature on the particle morphology was observed by performing experiments at 40°C, 50°C, 60°C and 70°C. The results are summarized in Table 1.

Table 1 Effect of temperature in the precipitation chamber on particle morphology

Temperature (°C)	Morphology
40	Coalescent particles
50	Spherical particles
60	Irregular shaped particles
70	Irregular and large crystals

At a precipitation temperature of 40°C, particle coalescence was observed. This can be explained considering that low precipitation temperatures can induce a partial solvent recondensation on the precipitated particles. Even in small proportions, the presence of solvent on the particles surface affects the interparticle forces, reducing the interparticle distance. Strong boundary forces, resulting from the surface tension of the solvent, can draw the particles together generating coalescence (Rhodes 1999). A better process performance was obtained by maintaining the precipitation chamber at 50°C for which more separated spherical particles than those produced at 40°C were observed. At temperatures of 60°C and 70°C, irregular shaped particles and large crystals were observed. The greater the temperature in the precipitation chamber, the greater is the tendency of the GF particles to form larger crystals. All these experiments were performed injecting GF concentrations of 15 mg mL^{-1} in acetone.

Effect of solute concentration

Systematic experiments were performed at different GF concentrations in acetone: the solute concentration was varied from 5 to 25 mg mL^{-1}. In all these experiments GF precipitated as spherical well-defined micrometric particles. Examples of this particle morphology are given in Figure 2. These SEM images refer to GF particles produced at solute concentrations of 15 and 25 mg mL^{-1}. Because they are reported with the same magnification, a qualitative evaluation of the particle size increase as the solute concentration increases is possible.

The particle size distribution of GF obtained at concentrations of 5, 15 and 25 mg mL^{-1} is given in Figure 3, and confirms the qualitative analysis based on the observations of Figure 2. Standard deviations were calculated for all the particle size distributions obtained and their values increased from 0.2 and 0.5 to 0.7 for particles obtained at 5 mg mL^{-1}, 15 mg mL^{-1} and 25 mg mL^{-1}, respectively. Particle size distributions were calculated from SEM images on the basis of the number of particles, then converted in terms of volumetric distributions and plotted in a cumulative form. The number of particles having a fixed diameter is not particularly relevant, since the weight of the drug with a given particle size is the key parameter with respect to therapeutic performance. The cumulative representation is also proposed since it better describes the contribution of the particles in terms of quantity of drug having a given size, because the volume, and not the diameter, is the relevant distribution parameter. Moreover, cumulative particle size distributions give a further indication: GF particles produced at 15 mg mL^{-1} strictly range from 0.5 to 3.5 μm. Therefore, this product seems the most appropriate in order to obtain a more efficient formulation.

The effect of GF concentration on particle size and distribution also reveals the possibility of particle tailoring depending on the target size requested (i.e. it is possible to control GF particle size by adjusting this SAA process parameter).

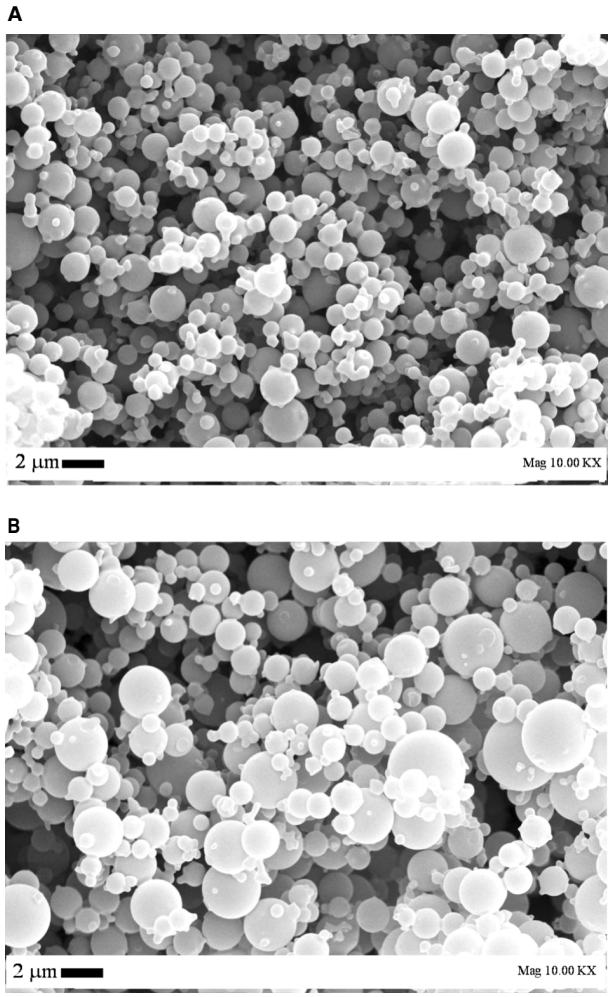

Figure 2 Scanning electron microscopy images of griseofulvin precipitated by supercritical assisted atomization from acetone, varying the solute concentration: A, 15 mg mL^{-1}; B, 25 mg mL^{-1}.

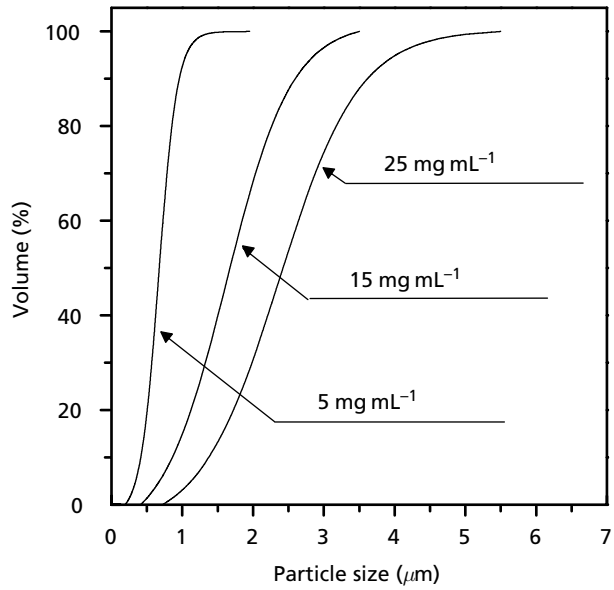

Figure 3 Cumulative particle size distributions (based on particle volume) of griseofulvin produced by supercritical assisted atomization varying the solute concentration in the solution.

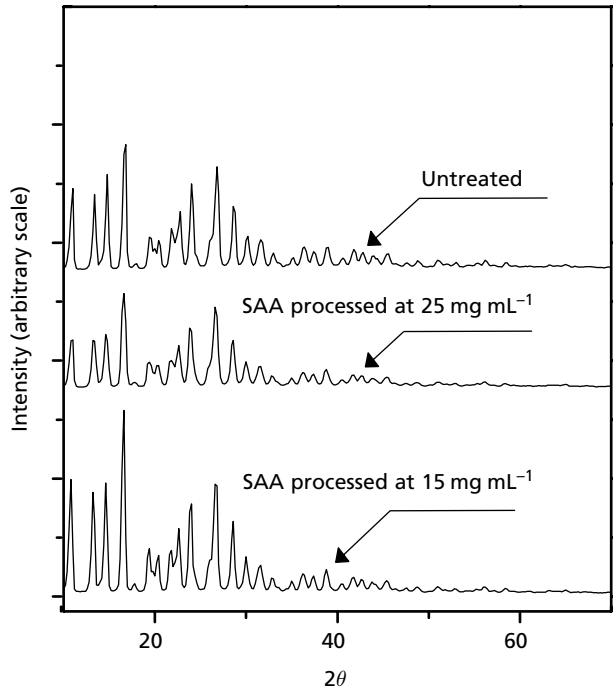

Figure 4 X-ray diffraction trace of untreated griseofulvin and supercritical assisted atomization (SAA) processed griseofulvin with a solute concentration of 15 and 25 mg mL^{-1}.

Micronized GF characterization

HPLC analyses were performed to evaluate if GF degradation occurred after SAA processing. HPLC traces of untreated and SAA-processed GF showed in all cases a single peak monitored after 26.4 min. Therefore, no GF degradation occurred during the SAA processing.

Headspace-GC-FID analyses measured in all cases an acetone residue of less than 800 ppm in the SAA-treated GF. This value is well below the International Conference on Harmonisation (ICH) limit, which is fixed at 5000 ppm (Federal Register 1997; ICH 1997).

The spherical shape of SAA-micronized GF particles could indicate an amorphous solid state, but in some cases we observed by SAA the formation of spherical particles formed by smaller crystals (Reverchon & Spada 2004). Therefore, to evaluate the solid state of unprocessed GF and of SAA-micronized GF, we performed some X-ray analyses. An example of the results obtained is given in Figure 4. X-ray diffraction traces revealed that micronized GF retains the crystalline structure after SAA processing (Figure 4).

SEM images obtained at greater magnification confirmed the substructure of the GF particles that are

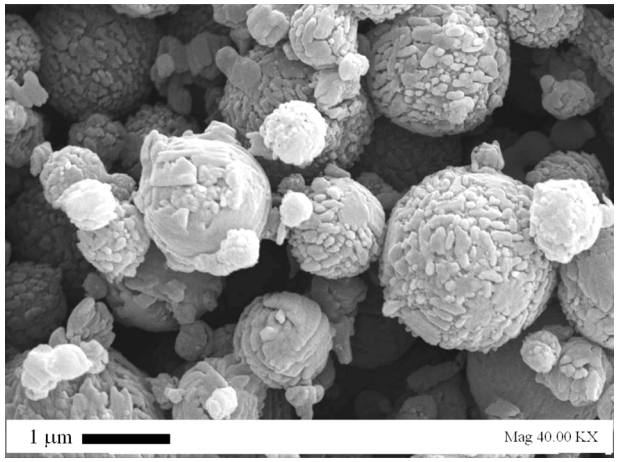

Figure 5 Scanning electron microscopy image of griseofulvin particles showing elongated crystals aggregates on the surface. The overall original spherical shape of the liquid droplets was maintained.

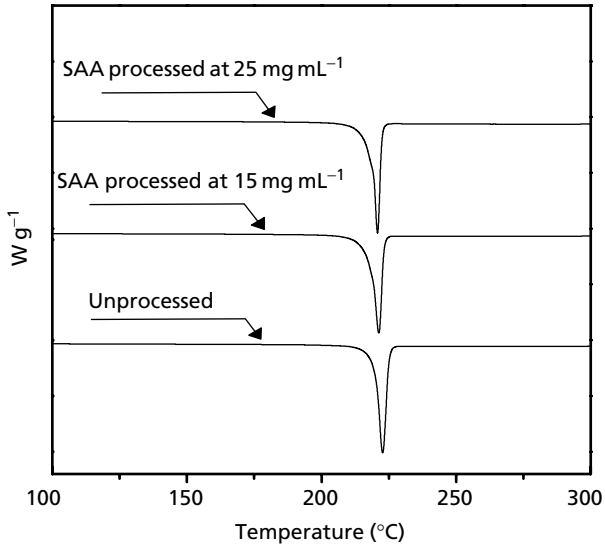

Figure 6 Differential scanning calorimetry traces obtained from different batches of supercritical assisted atomization (SAA) micronized griseofulvin. The trace of unprocessed griseofulvin is also given for comparison.

formed by submicrometric elongated crystals. An example of this structure is given in Figure 5, which shows GF nanocrystals confined in the spherical shape of the liquid droplets produced during the SAA atomization process. Recently, Reverchon & Spada (2004) performed systematic X-ray analysis of some SAA-processed compounds and demonstrated that, depending on the process conditions and the chemical structure of the treated compounds, it is possible to obtain crystalline microparticles retaining the spherical shape of the secondary droplets produced during the supercritical enhanced atomization.

The crystalline degree of SAA-processed GF was evaluated by DSC, considering that no polymorphism exists in this case (Ahmed et al 1998). In Figure 6, the results of DSC analyses performed on GF microparticles are proposed for particles produced at different solute concentrations in acetone to assess if this process parameter affects the crystalline habit of the drug. The DSC trace of unprocessed GF is also given for comparison. DSC traces show a well-defined endothermic peak located at 218°C for all the batches considered and a fusion enthalpy ranging from 118 to 122 J g^{-1} for the treated drug; a fusion enthalpy of 124 J g^{-1} was measured for the unprocessed drug.

These values were used to calculate the crystalline degree of SAA-processed GF. Assuming that raw GF is completely crystalline, the crystalline percentage was calculated as the ratio between the fusion enthalpy of the SAA-processed sample and the untreated GF sample. The results obtained for two different SAA-micronized GF batches, named B1 and B2, are given in Table 2. B1 was formed by GF particles produced at 25 mg mL^{-1} and had a crystalline percentage of 95%. B2 was formed by GF particles produced at 15 mg mL^{-1} and had a crystalline percentage of 90% (see Figure 4 for particle size distributions). B1 and B2 were analysed again by DSC after 6 days of storage in air with a relative humidity of 60%. The crystalline percentages calculated after storage are given in Table 2 and indicate no relevant variations of the crystalline habit. Results of the statistical analysis performed on the samples are also reported in Table 2. No statistical differences in the melting points were found; whereas a statistical difference in the fusion enthalpy between the untreated GF and the SAA-processed GF was observed. No relevant variations in the micronized powder morphology were observed by SEM after 6 days of storage.

Table 2 Percentage crystallinity of supercritical assisted atomization (SAA) precipitated powders (after SAA treatment and after 6 days of storage in air with 60% relative humidity) calculated from differential scanning calorimetry data according to the method proposed by Ahmed et al (1998)

Sample (no. of replicates)	Melting point			Fusion enthalpy			Crystallinity		
	°C	s.d.	NK	J g^{-1}	s.d.	NK	%	s.d.	NK
Untreated (3)	219.7	1.6	a	−124.4	5.4	b	100	–	a
GF 1 SAA (3)	219.8	1.6	a	−118.3	2.2	ab	95.1	2.6	ab
GF 1 SAA after storage (3)	219.5	3.1	a	−119.6	2.9	ab	96.2	2.4	ab
GF 2 SAA (3)	220.5	1.2	a	−113.1	1.5	a	91.0	3.1	b
GF 2 SAA after storage (3)	219.0	2.0	a	−114.2	1.5	a	91.8	3.8	b

GF, griseofulvin; NK, Newman–Keuls test: for each variable, values followed by different letters are statistically different (significance level = 0.05).

The proposed method to evaluate the crystalline degree is not rigorous. Indeed, Saleki-Gerhardt et al (1994) demonstrated that the DSC lower detection limit is

between 5% and 10% of the amorphous content. However, even in the case of maximum deviation (10%) between the measured percentages and the real value, the most important result is that the SAA-micronized GF retained its crystalline habit after 6 days of storage. Ahmed et al (1998) demonstrated that re-crystallization for partially amorphous GF takes place in about 6 h. Thus, it is possible to say that SAA-micronized GF showed good stability.

Surface area and dissolution tests

The surface area was measured for batches B1 and B2 (described above). A surface area of $4.22\,m^2\,g^{-1}$ was measured for B1 and a surface area of $6.15\,m^2\,g^{-1}$ was measured for B2; the unprocessed GF surface area was $0.87\,m^2\,g^{-1}$. The difference in surface area between samples B1 and B2 can be explained by considering that the mean diameter of B2 particles was less than that measured for B1; therefore a higher surface area was expected. The increase of one order of magnitude of the surface is a good result in view of the increase in drug bioavailability. For this reason, the GF sample B2, having the greatest surface area, was used for capsule preparation.

Gelatine capsules were prepared by mixing GF (conventionally jet-milled sample and B2 sample) with maize starch and were used for the dissolution study to better understand the behaviour of the formulated drug. Examples of the dissolution profiles of the SAA-micronized GF and the jet-milled drug are given in Figure 7, where the percentage of the dissolved drug is plotted against time. The experimental data in Figure 7 were obtained as the mean value of six repeated dissolution tests. This procedure was adopted because a single dissolution profile can show weak reproducibility owing to the manual preparation of the gelatine capsules. However, we noted that SAA-micronized GF showed a very uniform and repetitive dissolution profile, whereas the jet-milled drug showed a larger variability in the dissolution profile. This result indicates an advantage of SAA-processed GF over the jet-milled GF. Moreover, this behaviour is probably caused by the wider particle size distribution of the jet-milled GF with respect to the SAA-micronized drug.

The dissolution profiles revealed that more than 98% of the SAA-treated GF dissolves in 60 min, whereas only 75% of the jet-milled sample is dissolved in the same time. The percentages of drug dissolved at 60 min for SAA and jet-milled GF were also examined using the Mann–Whitney *U*-test and a *P* value of 0.02 was obtained (i.e. the difference between the percentages dissolved of SAA-treated and jet-milled GF at 60 min was statistically significant). These results confirm that the dissolution of SAA-treated GF is significantly faster than that of the jet-milled drug and that SAA micronization has the potential to improve GF bioavailability.

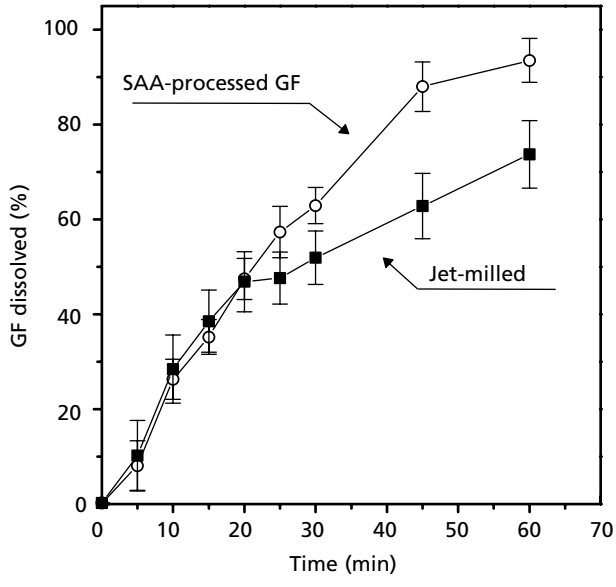

Figure 7 Dissolution profiles of supercritical assisted atomization micronized griseofulvin (GF) and conventional jet-milled GF (gelatine capsule).

References

Ahmed, H., Buckton, G., Rawlins, D. A. (1998) Crystallization of partially amorphous griseofulvin in water vapour: determination of kinetic parameter using isothermal heat conduction microcalorimetry. *Int. J. Pharm.* **167**: 139–145

Bleich, J., Kleinebudde, P., Muller, B. W. (1994) Influence of gas density and pressure on micropaticles produced with the ASES process. *Int. J. Pharm.* **106**: 77–84

Chang, C. J., Day, C.-Y., Ko, C.-M, Chiu, K.-L. (1997) Densities and P-x-y diagrams for carbon dioxide dissolution in methanol, ethanol, and acetone mixtures. *Fluid Phase Equilibria* **131**: 243–258

Chattopadhhyay, P., Gupta, R. B. (2001) Production of griseofulvin nanoparticles using supercritical CO_2 antisolvent with enhanced mass transfer. *Int. J. Pharm.* **228**: 19–31

DeGioannis, B., Jestin, P., Subra, P. (2004) Anti-solvent and co-solvent effect of CO_2 on the solubility of griseofulvin in acetone and ethanol solutions. *J. Supercrit. Fluids* **29**: 49–57

Federal Register (1997) Vol. 62 No. 247, December 24

Foster, N. R., Meure, L. A., Barrett, A. M., Abbasi, F., Dehghani, F. (2003) Micronisation of griseofulvin by the aerosol solvent extraction system. In: Brunner, G., Kikic, I., Perrut, M. (eds) *Proceedings of the 6th International Symposium on Supercritical Fluids*, Versailles. International Society for the Advancement of Supercritical Fluids, Nancy, France, pp 1771–1776

Gull, K., Trinci, A. P. J. (1973) Griseofulvin inhibits fungal mitosis. *Nature* **244**: 292–294

ICH (1997) *Q3C: Impurities: Guideline for residual solvents*. Step 4. ICH, Switzerland

Kerc, J., Srcic, S., Knez, Z., Sencar-Bozic, P. (1999) Micronization of drugs using supercritical carbon dioxide. *Int. J. Pharm.* **182**: 33–39

Lin, C., Magat, J., Chang, R., McGlotten, J., Symchowicz, S. (1973) Absorption, metabolism and excretion of griseofulvin in man. *J. Pharmacol. Exp. Ther.* **187**: 415–422

Liu, H. (1999) *Science and engineering of the droplets. Fundamentals and application*. William Andrew Publishing, New York

Matson, D. W., Fulton, J. L., Petersen, R. C., Smith, R. D. (1987) Expansion of supercritical fluid solution: solute formation of powders. Thin films and fibers. *Ind. Eng. Chem. Res.* **26**: 2298–2306

Mosharraf, M., Nystrom, C. (1995) The effect of particle size and shape on the surface specific dissolution rate of micronized practically insoluble drugs. *Int. J. Pharm.* **122**: 35–47

Ohe, S. (1990) *Vapour-liquid equilibrium data at high pressure*. Elsevier, Amsterdam

Quanyun, A. X., Lawrence, A. T. (1999) *Stability indicating HPLC methods for drug analysis*. Pharmaceutical Press, London

Rehman, M., Shekunov, B., York, P., Colthorpe, P. (2000) Crystallisation of an inhalation compound in supercritical fluids: optimization of particulate and solid properties. *J. Pharm. Pharmacol.* **52**: 27–30

Reverchon, E. (2002) Supercritical assisted atomization to produce micro and/or nano particles of controlled size and distribution. *Ind. Eng. Chem. Res.* **41**: 2405–2411

Reverchon, E. (2003) Process for production of micro and/or nano particles. Patent no. WO 03004142

Reverchon, E., Della Porta, G. (1999) Production of antibiotic micro- and nano-particles by supercritical antisolvent precipitation. *Powder Technol.* **106**: 23–29

Reverchon, E., Della Porta, G. (2003a) Micronization of some antibiotics by supercritical assisted atomization. *J. Supercrit. Fluids* **26**: 243–252

Reverchon, E., Della Porta, G. (2003b) Terbutaline microparticles suitable for aerosol delivery produced by supercritical assisted atomization. *Int. J. Pharm.* **258**: 1–9

Reverchon, E., Della Porta, G. (2003c) Particle design using supercritical fluids. *Chem. Eng. Tech.* **8**: 840–845

Reverchon, E., Spada, A. (2004) Crystalline microparticles of controlled size produced by supercritical assisted atomization *Ind. Eng. Chem. Res.* **43**: 1460–1465

Reverchon, E., Della Porta, G., Taddeo, R. (1995) Solubility and micronization of griseofulvin in supercritical CHF_3. *Ind. Eng. Chem. Res.* **34**: 4087–4091

Reverchon, E., Della Porta, G., Spada, A. (2003) Ampicillin micronization by supercritical assisted atomization. *J. Pharm. Pharmacol.* **55**: 1465–1471

Rhodes, M. (1999) *Introduction to particle technology*. Wiley & Sons, New York

Saleki-Gerhardt, A., Ahlneck, C., Zohografi, G. (1994) Assessment of disorder in crystalline solids. *Int. J. Pharm.* **10**: 135–144

Sellers, S. P., Clark, G. S., Sievers, R. E., Carpenter, J. F. (2001) Dry powders of stable protein formulation from aqueous solutions prepared using supercritical CO_2 assisted atomization. *Pharm. Sci.* **90**: 785–797

Sencar-Bozic, P., Srcic, S., Knez, Z., Kerc, J. (1997) Improvement of nifedipine dissolution characteristics using supercritical CO_2. *Int. J. Pharm.* **148**: 123–130

Sievers, R. E., Milewski, P. D., Sellers, D. P., Kusek, K. D., Kleutz, P. G., Miles, B. A., (1998) Supercritical CO_2-assisted methods for the production and pulmonary administration of pharmaceuticals aerosol. *J. Aerosol Sci.* **29**: 1271–1272

Subramaniam, B., Rajewski, R. A., Snavely, K. (1997) Pharmaceutical processing with supercritical carbon dioxide. *J. Pharm. Sci.* **86**: 885–890

Turk, M., Hils, P., Helfgen, B., Schaber, K., Martin, H. J., Wahl, M. A. (2002) Micronization of pharmaceutical substances by the rapid expansion of supercritical solution (RESS): a promising method to improve bioavailability of poorly soluble pharmaceutical agents. *J. Supercrit. Fluids* **22**: 75–84

Ventosa, N., Sala, S., Torras, J., Llibre, J. (2001) Depressurization of an expanded liquid organic solution (DELOS): a new procedure for obtaining submicron- or micron-sized crystalline particles. *Crystal Growth Des.* **1**: 299